RESEARCH NOTE

DESIGN AND CONSTRUCTION OF A SENSITIVE CAPACITIVESENSOR SYSTEM

H. Golnabi

Institute of Water and Energy
Sharif University of Technology
Tehran, Iran

(Received: Dec. 5, 1996 - Accepted in Revised Form: Feb. 4, 1999)

Abstract Design and construction of a capacitor sensor with a precise readout system are described in this paper. A variable air-gap capacitive transducer was constructed and for signal measurement a successful attempt was made to exploit the capacitance changes in terms of the phase angle of the detected signal. The reported setup makes it possible to detect capacitance changes of the order of 2.5 fF in a 4.5 pF range and the readout circuit can detect a capacitance change of about 22 aF (5 in 10^6). There is a linear relation between the air-gap distance and the output of the sensor over an experimented gap range of 0.5-4.5 mm. It shows a nonlinearity deviation factor of 1% from the expected theoretical line. The dynamic range of the system is variable from 5 Mm to 2.5mm and it mainly depends on the initial air-gap distance. Adding a stray capacitance of 180 pF to the system only causes a 0.1% error in the sensor output. In comparison with the other sensor systems the one reported in this paper is much more sensitive, reliable, and stray-immune to electrical interferences.

Key Words Design, Capacitor, Sensor, Readout Circuit

t BwA o ,o¢ve S i Bw /SwA ²k{ x nq£ · ¼j »¯pB i o¢ve ð ½ S i Bw ° »e¥o¥ ³$B¸« ËA nj **²k¼ña** ²k{ ²jB´TwA pBµ o¼°U ³ ¬pB i S¼µo© o¼°U x °n pA ,ºo£²pAk¯A nAk« S i Bw ºo ° ²j±o¼°T« ² Bñ{ B ¬pB i ±ñ¼QQ 4.5 ¬pB i S¼µo© ºo - jAnBµ ±Ta µ 2.5 j°ke - ð a±½ »¯pB i Ro¼°U ,o¢ve ËA pA ²jB´TwA B /SwA oÇA ,oTa¼¦¼Ç« 4.5 - å.5 ² BÇñ{ ·¦æBÇµ ºoÇ ° ²j±Ç »¤i ,o¢ve ËA »]°oi /SwA ²k{ ºo£²pAk¯A jAnBµ »Un±~ »e¥o¥ /SwA oTa¼¦¼« 2.5 B ¬°oñ¼« 5 pA ,©Tv¼w ËA ºnB½¶j°kd« /SwA kænj ð ½ pA oTa½ »¤i o½± kænj å.1 B´ U ºjAnBµ ±ñ¼Q 18å »µB¡A ¬pB i ð ½ ¬j°qµA ° ²j± q¼aB¯ ©Tv¼w o S¼phBQ ºB´¯pB i oA ³½ SwA /k½»« jB\A »]°oi nj B¤i

INTRODUCTION

Much progress has been made over the last few years in developing the capacitor transducers [1-4] and complementing measuring circuits [5,6]. However, for the precision in instrumentation and measurements, the capacitances to be measured are in the range of 0.1-10 pF with a required resolution of better than 0.1-10 fF, respectively. This requirement along with other considerations such as environmental effects and structural stability challenges the development of a much more sensitive capacitive sensor system. To alleviate some of the problems a sensitive sensor system was developed of which the results are reported in this paper.

In order to have a reliable sensor system several parameters should be taken into account its design and its operation. Regarding the transducer part, high structural stability, sensitivity, flexibility, and dynamic range of operation are important. In fact parameters such as sensitivity, stability, and immunity to stray capacitances have encouraged the development of the new readout circuits. The

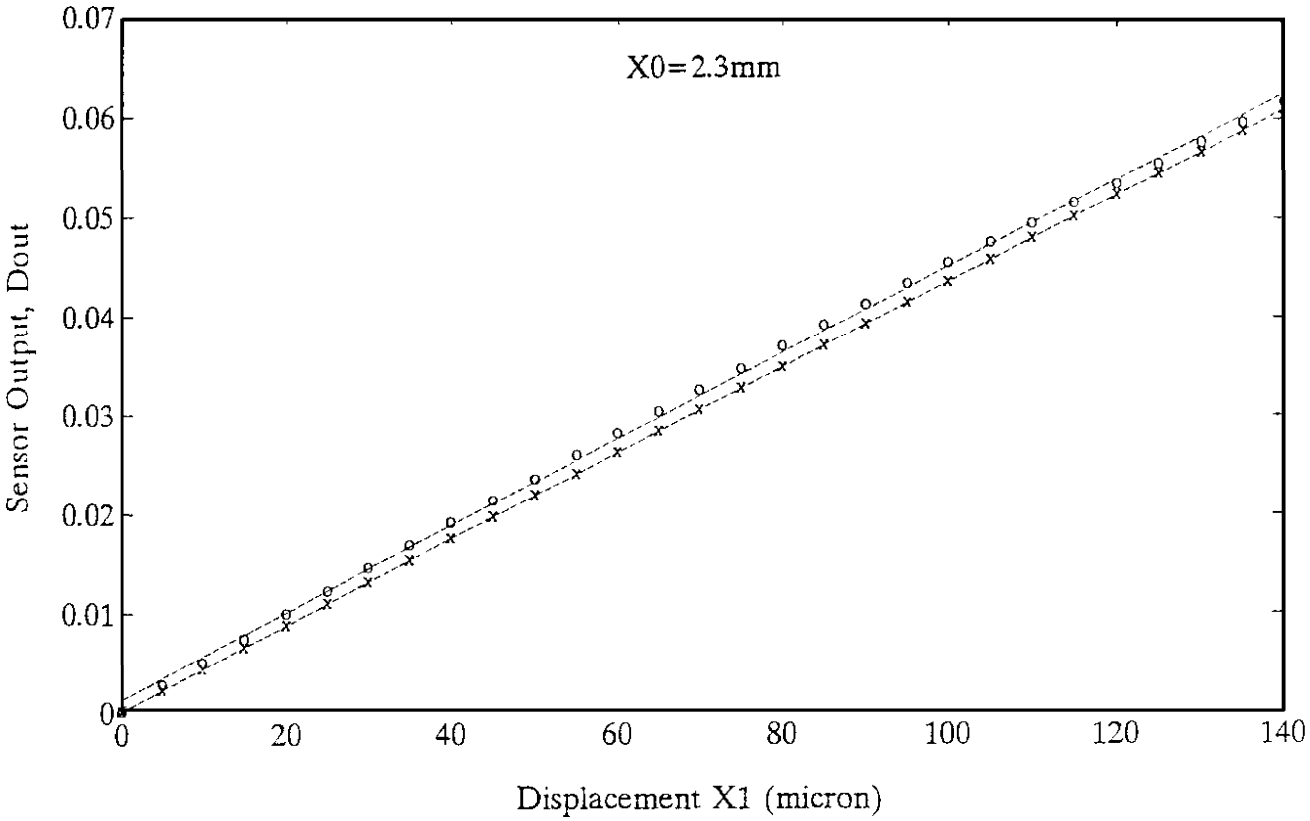

Figure 1. Cross-sectional view of the capacitive transducer. The main components are the upper electrode (50 mm diameter and 2 mm thickness), a lower electrode (25mm diameter and 2mm thickness) with a guard-ring (outer diameter 50mm and inner diameter 26mm), the lower and upper electrode supports (82mm diameter and 8mm thickness), three adjusting screws (M5, 30mm length), three springs, and a micrometer screw.

complexity of the readout circuit and the system cost are the other important factors which play key roles in the sensor mass production and in the real field applications.

In this paper, first, we describe the design and construction of the transducer and the readout detection circuit. The mechanical details of the designed sensor is given and its operational advantages and disadvantages are discussed. In the detection part, the electrical characteristics of the readout circuit are presented and the operation of the new setup for measuring the capacitive changes is demonstrated. Second, we present the experimental results with more emphasis on the special features of the reported system. Finally, we conclude thes paper by giving a summary of the results and making some suggestions for further improvement of the system.

TRANSDUCER DESIGN

A schematic cross section of the designed transducer is shown in Figure 1. The basic instrumentation associated with this type of transducers is simple and requires only a variable gap capacitor, a mechanical mount, and a drive mechanism to change the air-gap distance.

The main body of the unit consists of two pieces of plexiglasses as shown in Figure 1. These two plates are machined carefully and connected together by three spring loaded

screws. By using these screws the coarse spacing between the two plexiglass plates is controllable. In practice, it is possible to change the distance between the capacitor main electrodes and also to check the parallelism of the electrodes with respect to each other.

The capacitor electrodes are machined from brass or aluminum rods. The upper electrode has a diameter of about 50mm and a thickness of about 2mm. This electrode plate is mounted on another piece of plexiglass which has a diameter of about 55mm. Actually this is the moving electrode of the capacitor and is connected to a micrometer screw.

The lower electrode of the capacitor consists of an inner electrode plate with a diameter of 25mm and a Kelvin guard-ring [7,8] with the outer diameter of 50mm. The two electrodes are carefully mounted on a plexiglass piece. The gap provided between the inner electrode and the guard-ring is about 0.5mm thick which is from the plexiglass material. Two electrodes have a thickness of about 2mm. Like the other electrode these electrodes are carefully machined from the aluminum rod and are polished for a good surface quality.

The error sources in the transducer design and operation can be the guard- electrode, gaps, sensitivity to electrode distance variation, sensitivity to lateral displacement, tilt and bending of the electrodes, electrode contamination, and the gap dielectric condition.The gap condition includes the dielectric variation due to humidity, temperature, and the absorptin effect. In our design we have considered all these parmeters and care has been taken to minimize these errors during both construction and measurements.

For a more precise linear positioning a stepping motor is connected to the micrometer screw by a flexible coupler. With a 500 mm/turn screw pitch and a motor with 800 steps/turn (Step-Syn model number 103-7550-0110) it is possible to have a minimum step size of about 0.625 mm in the displacement measurements. For automating the system, an interface board is designed which controls the motor movement. A fine movement of the capacitor electrode and as a result a precise control of the capacitor gap distance are accomplished by this hardware-software combination.

DESCRIPTION OF THE READOUT CIRCUIT

Several techniques such as resonace, oscillation, charge/discharge and AC bridge are used in many applications. For detecting signal, we have taken the advantage of a new technique which is based on the capacitance-to-phase angle conversion[9,10]. The schematic representation of the readout circuit is shown in Figure 2a, which requires a circuit design for producing two signals with an appropriate phase difference($\pi - \gamma$). This ciruit design is not shown in Figure 2a but can be found in references[9,11]. More details of producing two sinusoidal input signals can be found in Ref.[9], where the phase angle γ in determined from $\tan^{-1}(R_1 C_1 \omega)$. For the operating frequency of 10kHz, R_1=1k Ω and C_1=10nF the phase angle γ is about 3.67 degrees. The amplitude of these signals A and B, Figure 2b, is about 5 V which is adjustable for one of the input signal (in this case A).

Other components are a buffer amplifier, comparators, low pass filters, analog with the digital converters, and digital to analog converters. Figure2b shows the arrangement of the stray capacitance measurements. If C_x is an unknown capacitance then this technique can be used to measure any small changes on its capacity (ΔC_x). Also by placing a well defined capacitance C_0 in parallel with C_x one is able to

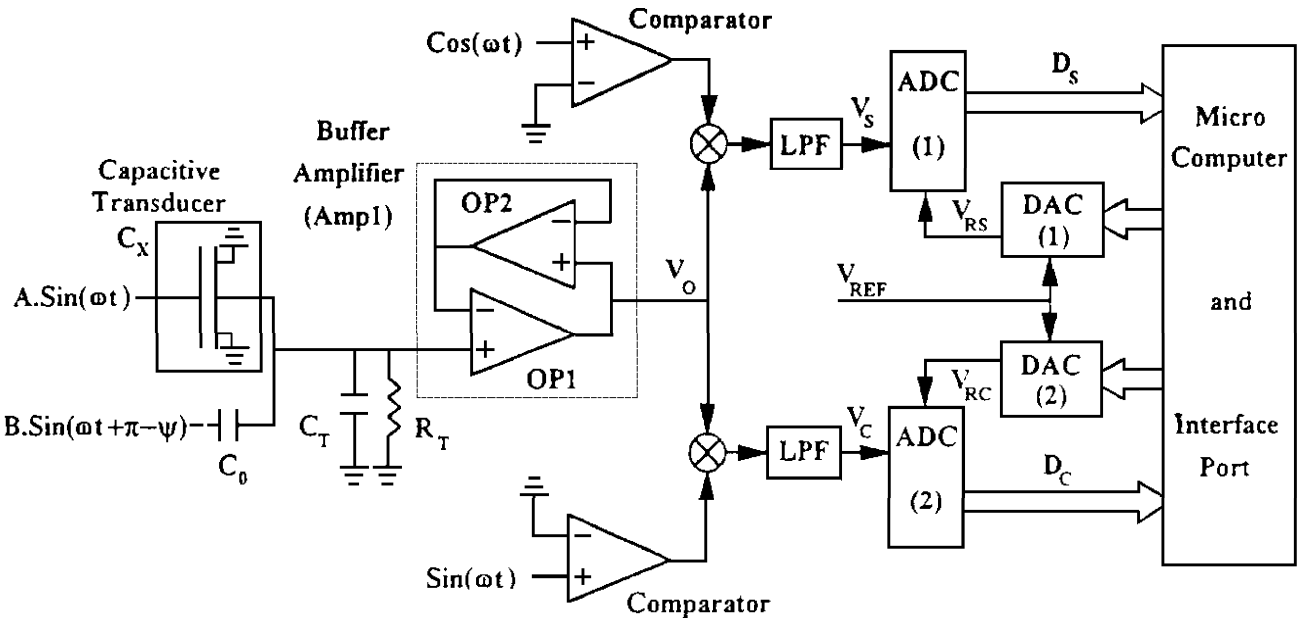

(a)

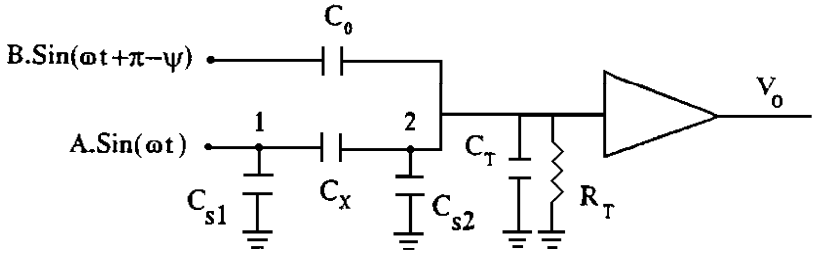

(b)

Figure 2. (a) Schematic block diagram of the readout and the monitoning circuits. The main components are a capacitive transducer, C_x (variable from. 75 pF to 9 pF), a reference capacitor C_0 (12 pF, 24 pF or 34 pF), C_T(12 pF) and R_T(22 MW), a buffer amplifier (OP1 and OP2, LF 353), two comparators (LM319), two low pass filters (f_0= 2 Hz), two ADCs (ICL 7109), two DACs (DAC0800), interface board, and a PC for signal processing. (b) C_{s1} and C_{s2} are the stray capacitances (180 pF) added alternatively to the circuit at node 1 or 2.

measure the value of the Cx with a high accuracy.

Alternatively, we can measure a normalized capacitance ratio such as C_x/C_{x0}, where C_{x0} is are ference value for C_x and we define $C_x=C_{x0}+C_{x1}$. Here C_{x1} is the capacitance change of the transducer due to a displacement of X1 from its initial position, X_0. The block diagram of the detection and monitoring system is also shown in Figure 2a. As can be seen, the final signal is processed digitally by a PC, while the output is recorded as a dimensionless number.

Following the theoretical analysis given in Reference [9], the normalized digitized output, D_{out}, can be written as

$$D_{out} = \frac{C_{x1}}{C_{x0}} = \frac{\tan(\Upsilon)}{n}\frac{D_c}{D_s} \qquad (1)$$

where, Υ is the phase difference, D_c and D_s are

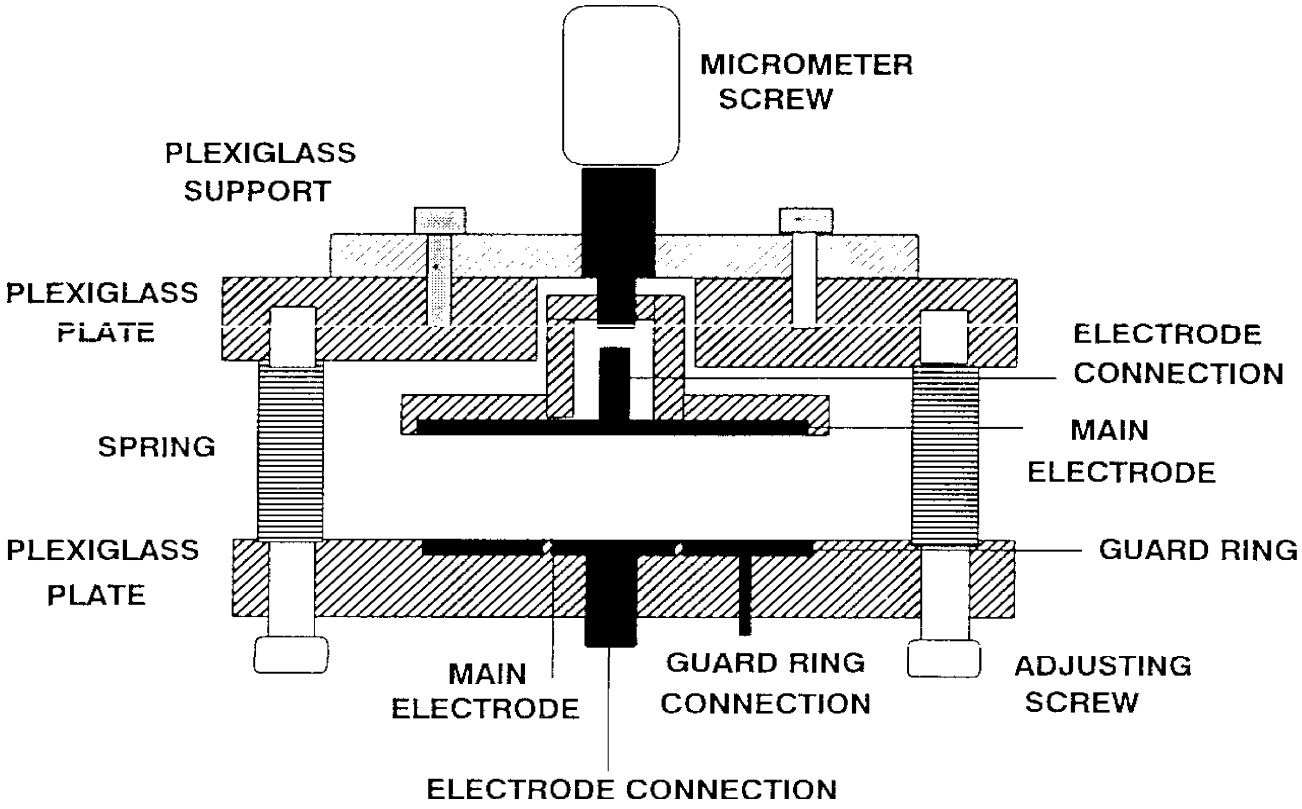

Figure 3. Variation of the sensor output with respect to the displacement for X_0=2.3mm. The line denoted by, o, is for the experimental results and by, x, is for the theoretical calculations.

digitized output of two ADCs as shown in theblock disagram of Figure 2a, and n is the parameter that depends on the voltage ratio of the two multipliers (V_{RS}/V_{RC}).

Now any change in the value of C_{x1} such as DC_{x1} can produce variation in the output such as (for constant values of n and Y):

$$DD_{out} = \frac{DC_{x1}}{C_{x0}} = \frac{\tan(Y)}{n*2^{m-2}} \qquad (2)$$

where, m is the number of bits of the ADC and other parameters are defined previously. The parameter DC_{x1} can be considered as the minimum resolvable capacitance change (MRCC) of the reported readout scheme.

By substituting the capacitances in terms of the gap distances in Equation(1) and exchanging the positions of C_{x0} and C_0 in the circuit (see Figure 2a) the final equation for data analysis becomes.

$$D_{out} = X_1/X_0 \qquad (3)$$

where X_0 is the distance at which the zero adhustment is made and X_1 is the displacement from X_0. In fact Equation(3) shows the calibration line for the sensor system. The importance of this scheme is the linear relationship between the output signal and the parameters to be controlled (the gap distance in this case). Another advantage of this method is that output readout signal corresponding to the capacitance change is independent of the C_0 value. However, C_{x0} and as a result X_0 value control the slope of the calibration line in sensor operation.

EXPERIMENTAL RESULTS

Our experimental system consists of a

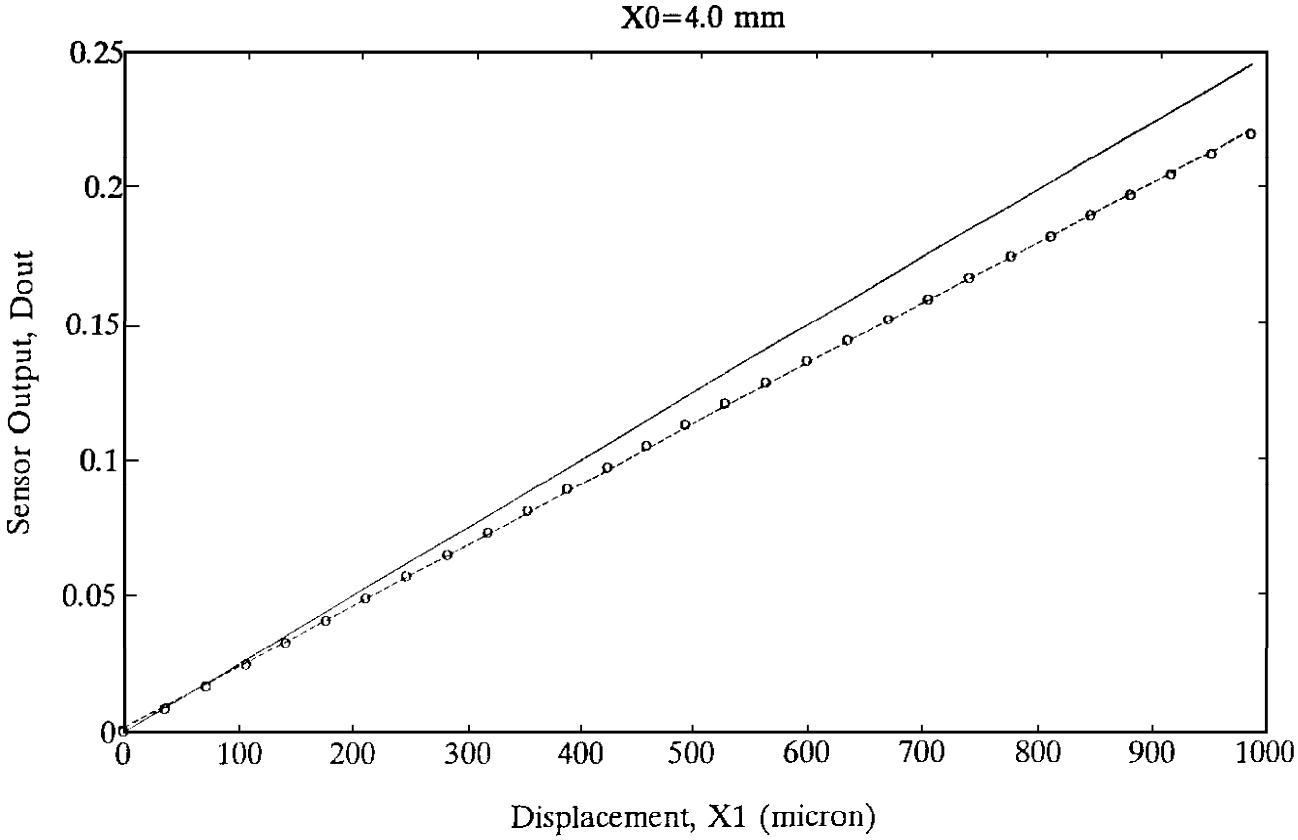

Figure 4. Sensor output as a function of displacement for X_0=4mm. The line denoted by, o, is the experimental results and the solid line shows the theoretical results.

transducer, a detection circuit, and finally a digital signal processing uint. By using the constructed transducer and readout circuit, data collection was accomplished by a PC via a written program to control both the stepper motor and the signal processing. In the first experiment the variation of the output, D_{out} with respect to the gap distance, X_0, was studied. The digitally averaged output values at different X_0 values were recorded and the result of this study for X_0= 2.3 mm is shown in Figure 3. To compare these results with the theoretical calculations, the experimental slope $1/X_0$ was computed through a least line fit method. The experimental slope is $4.38 * 10^{-4}$ which is in clear agreement with the theoretical slope of $4.35 * 10^{-4}$.

In order to determine the deviation of the experimental values from the expected theoretical values and as a result the linearity of the system we calculated the deviations at several X_0 values. In general this deviation or nonlinearity factor is of the order of 1%.

To check the linearity of the sensor at higher gap distances the output variation for X_0= 4mm is displayed in Figure 4. As can be seen in Figure 4 this sensor system shows a linear behavior at this value of X_0. The results of this study indicate that for this range of operation (X_0= 0.5-4.5mm) the linearity of the system is quite acceptable. However, by increasing X_0 one expects that the deviations of the output signals from the expected theoretical values increase. This nonlinearity could be due to two factors, one is the nonlinearity of the mechanical drive system and the other is the transducer

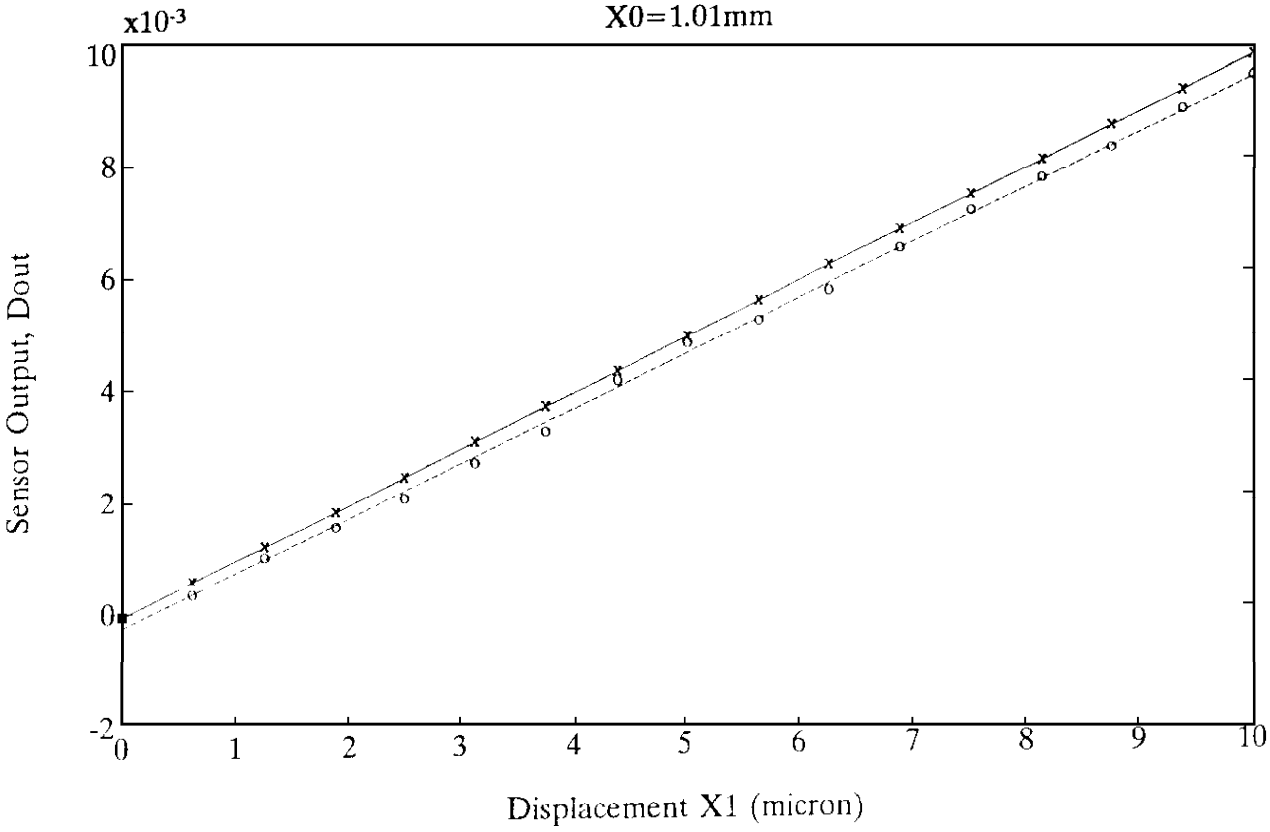

Figure 5. Sensor output variation as a function of displacement for X_0=1.01 mm to show the sensor resolution. The line denoted by, o, is the experimental results and the one denoted by, x, is the theoretical calculations.

(depends on the difference between the radius of the guard-ring and the inner electode with respect to the gap distance). At higher X_0 values the edge effects become more pronounced, thus the small nonlinearity can be explained by considering these factors.

To check the resolution of the system, in another study we have used the smallest single step scan (0.625mm) in the range of X_0= 1.01 mm (C_{x0}= 4.5pF). The result of this study, shown in Figure 5, indicates that the theoretical slope of this line is $9.9 * 10^{-4}$ corresponding to a resolution of about 5 in 10^{-6}. Comparing this resolution with 44 in 10^6 for X_0= 2.3mm and 127 in 10^6 for X_0= 4mm, one can observe that the resolution of the system is decreasd by increasing the X_0 value. Theoretically this can be noticed from Equation (3) in which DD_{out} is inversely proportional to X_0 and directly proportional to the DX_1. However, it would be noticed that although decreasing X_0 will considerably increase the sensitivity of the device, the dynamic range of its operation decreases. So depeneing on the application conditions, one can optimize the system for an appropriate operation range and resolution.

The variation of the capacitance change for X_0= 1 mm is presented in Figure 6. The minimum resolvable capacitance change (MRCC) of the readout circuit for C_{x0} value of about 4.5 pF is 22 aF. Theoretically MRCC can be obtained from Equation (2). Three parameters Y, n, and m influence the resolution of the readout circuit. To increase the resolution, one can increase n and m or change the phase angle Y. The overall resolution of the

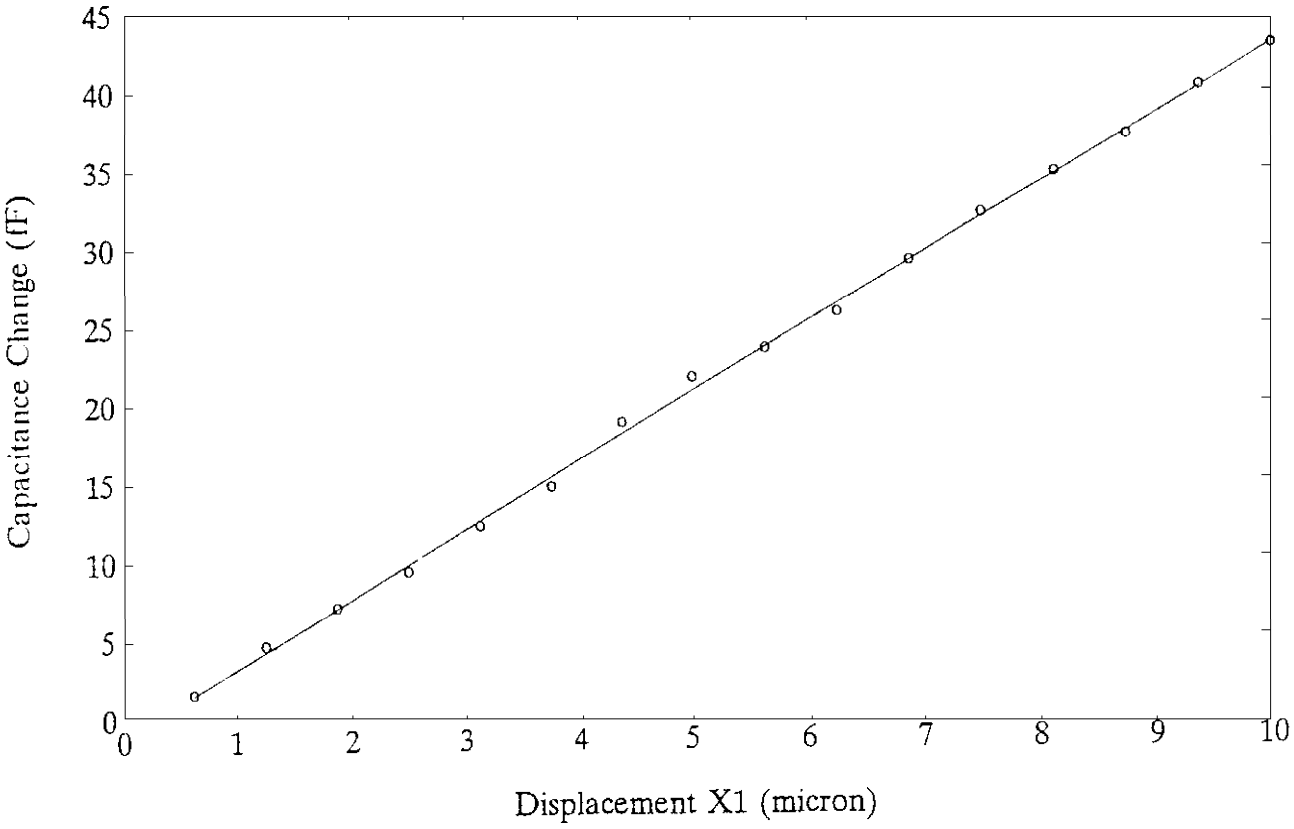

Figure 6. Capacitance changes as a function of displacement for C_{x0} value of about 4.5pF.

device is controlled in part by the mechanical drive system and the readout circuit. The minimum resolvable displacement for the mechanical drive unit is limited by the pitch of the micrometer screw and the number of motor steps per turn. Because of the low resolution of the mechanical drive system the overall resolution of the present system is limited to a cpacitace change of about 2.5 fF in 4.5 pF range (5.5 in 10^4). With the present combination a minimum displacement change of about 0.625 mm is possible. This value is much less than that of the readout system which is around 25 nm. However, the mechanical resolution can be reduced to the half of this value by driving the motor at half step mode of operaion.

Although increasing n increases the resolution, it decreases the dynamic range of the measurements. This is illustrated in Figure 7 for different n values which clearly shows the variation. As can be observed from Figure 7 the dynamic range is about 952.5 mm for n= 0.4 while it decreases to 7.5 mm for n= 7 (for X_0=2.3mm and Y=3.67 degree).

One of the most important parameters in the sensor performance is the reporducibility of the system. In order to test this parameter we plotted the results of the two different runs at the same value of X_0=4.28 mm. To see the data points better in Figure 8 intentionally we picked up the two runs with different scanning increments (one has an increment of 1.25mm and the other 1.875mm). As can be seen in Figure 8 there is a good agreement between the result of the two trials, which confirms the reproducibility of the system.

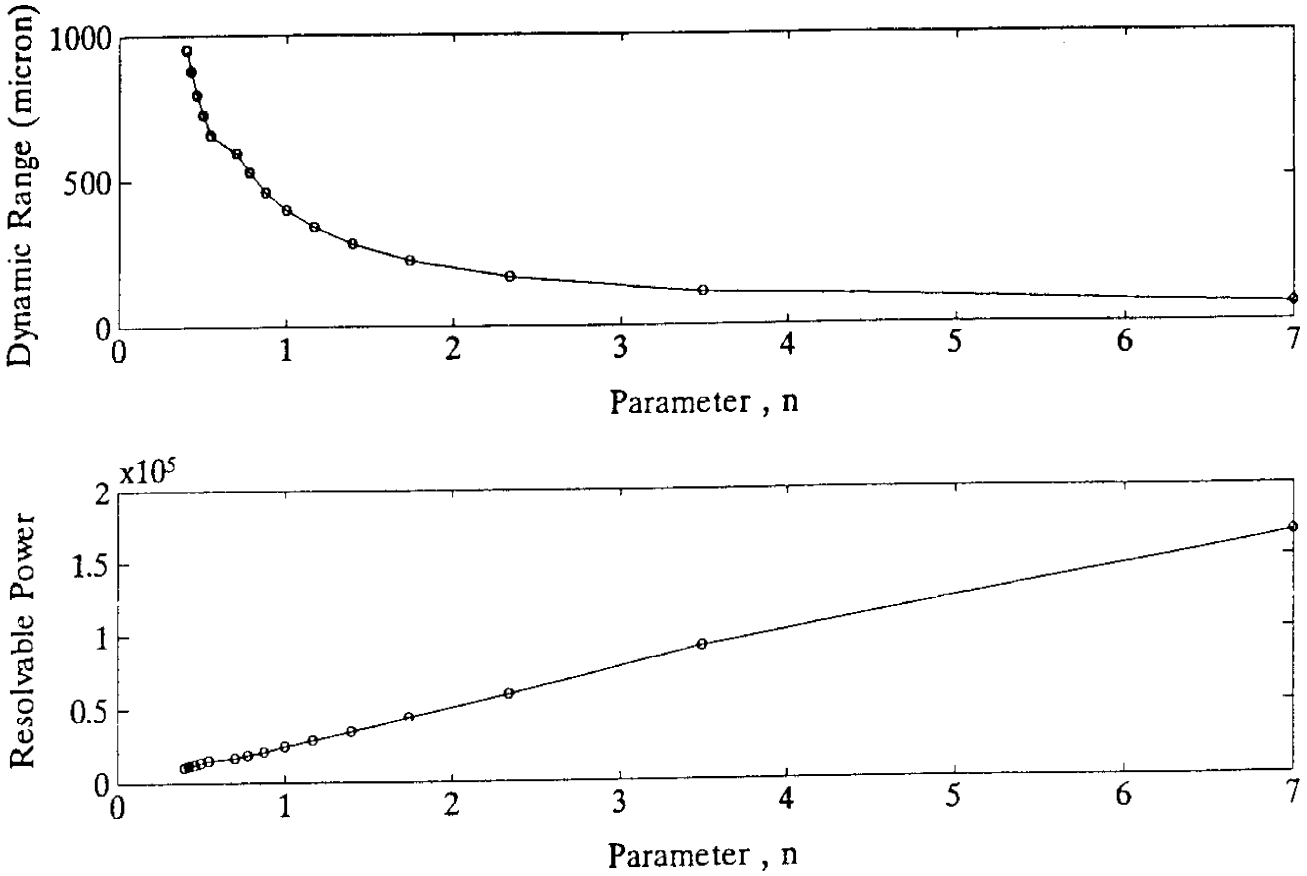

Figure 7. Sensor dynamic range as a function of parameter n at a fixed value of X_0=2.3mm, top. The bottom part shows the correspoding readout resolving power.

It should be mentioned that the experimental slope of the line denoted by symbol, o, is $2.9 * 10^{-4}$ while the slope of the other line is $2.84 * 10^{-4}$. As can be seen the difference in the slopes is only $0.06 * 10^{-4}$ which is negligible. However, the remaining difference is due to the zero adjustment (difference in the line intercepts) which could be corrected by the zero adjustment option of the readout system. This difference, however, does not have any effect on the slope of the calibration line, which is the more important parameter of the sensor system.

The effect of changing the value of the reference capacitance, C_0, (see Figure 2a) in the sensor output was studied for different capacities. The result of this study for C_0= 12 pF, 24 pF, and 34 pF are presented in Figure 9. Two inportant points can be concluded from the results of this study. First, the slopes of the calibration lines are $1.3 * 10^{-4}$, $9.9 * 10^{-4}$, and $9.6 * 10^{-4}$ for the case of C_0=12pF, and 24pF, and 34 pF, respecitvely. The slopes within the experimental error of the system ($0.4 * 10^{-4}$ at this range) are the same which means that the slope of the calibration line is independent of the C_0 value. This fact is in agreement with the outcome of Equation (3) which clearly shows that the final formula does not depend on the C_0 quantiy. Second, as can be seen in Figure 9, by increasing C_0 value the dynamic range of the operation also increases accordingly. The dynamic range for C_0= 12pF, 24pF, and 34pF are 170mm, 220mm, and 270 mm, respectively

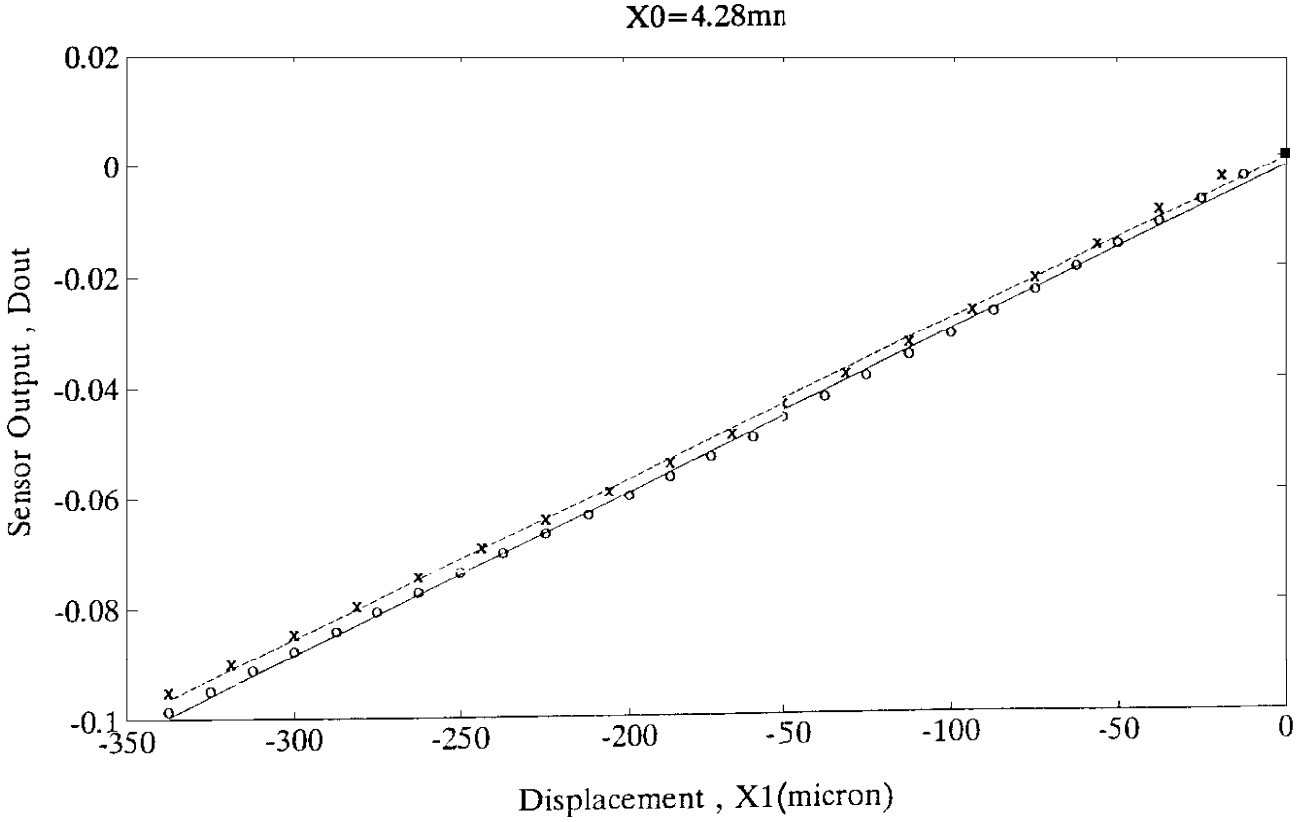

Figure 8. Sensor output readouts at the two different trials denoted by, x, and, o, to show the reproducibility of the system for a fixed value of X_0=4.28mm.

(X_0= 1mm). However, it should be mentioned that increasing the C_0 value will decrease the sensitivity of the detection system to some extent. So there is as usual a trade off between the system dynamic range and its sensitivity.

A comparison of the results of this study with those of others reported in the literature will reveal some of the featurs of the new system. A digital readout technique for capacitor sensor application has been reported[5] in which a capacitor difference with a resolution of 0.05 fF on capacitiors in the 20-100 fF range has been obtained. Later some attempts have been made in order to cancel the noise effect for the readout system. This readout circuit has been used for a pressure sensor chips containing 100 pF air - gap capacitors and a resolution in the 30 aF range has been reported[6].

In another study [12] the use of a long range capacitive displacement sensor is explained which has a resolution of 1mm over a wide range of about 150 nm. In comparison with this report our readout system has a resolution of about 25 nm and the transducer with 1 mm air-gap distance shows a resolution of about 5 ppm. The result of our prototype system reveals a high sensitivity and linearity at a reasonable mid dynamic range.

However, increasing the number of averaging points in data recording increases the resolution, but with the available ADCs it increases the measurement time. The resolution of the readout system is however much more than the resolution of the drive unit for the transducer. It must be pointed out that the design of capacitors with very small capacity is

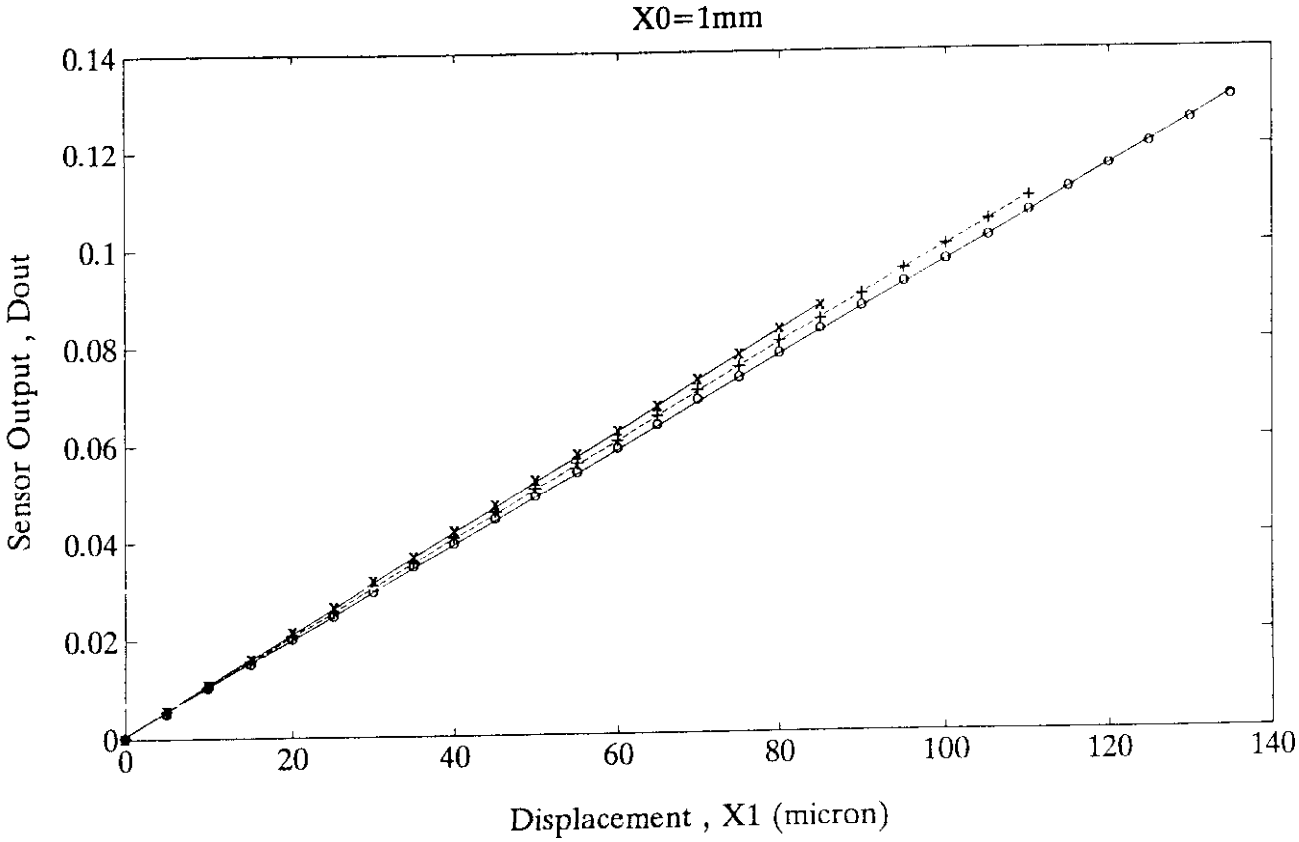

Figure 9. Shows the effect of varying C_0 in the sensor operation. The solid line denoted by the symbol, x, is for the case of C_0=12pF, the dashed-line denoted by, +, is for C_0=24 pF, and the one denoted by, o, corresponds to C_0=34 pF.

only possible in the integrated circuits and would be hard to build in a discrete fashion. The readout system reported here with a high sensitivity is very suitable for measuring such small capacitance changes in integrated circuits.

To check the stray immunity of the system, we have meaured the output changes due to adding the stray capacitances C_{s1} (node 1) orC_{s2}(node 2) as shown in Figure 2b. For adding C_{s1}= 180 pF the output change was about $1.88 * 10^{-3}$ which corresponds to a capacitance change of $8.46 * 10^{-3}$ pF for the C_{x0} value of 4.5pF. Placing C_{s2}=180 pF at node 2 the output variation is even less in the order of 10^{-3} ($4.5 * 10^{-3}$ pF) for the same C_{x0} value which indicaltes that the system is more immune to the stray capacitances from this side of the system.

If we define the stray immunity factor as DC_x/C_s then we can compare our results with those of the others[13]. In that report a stray immunity factor of 10^{-4} has been obtained (for C_s= 100pF) while our system shows a factor of $4.7 * 10^{-5}$ at node 1. The stray immunity factor as DC_x/C_s of $4.7 * 10^{-5}$ at node1. The stray immunity factor at node 2 for our system is $2.5 * 10^{-5}$ in comparison to $5 * 10^{-5}$ for that report which is better by a factor of 2.

CONCLUSIONS

In summary, there is a good agreement between the experimental results of this work and the calculated values for the system calibration line, resolution, and the operation range. Other advantages of this system are the reliability,

stability, and the stray-immunity which allows its operation in open environment without any shielding requirement. Although the results are satisfactory, the mechanical drive system can be further improved to increase the mechanical resolution and also to increase the dynamic range of the operation. The resolution of the readout circuit can also be improved by using high speed ADCs with higher bit numbers. Even though the capacitance changes were measured in this study, it is also possible to implement the reproted system for sensing other parameters that somehow have small influence on the tranducer capacity [14,15].

Error analysis of the reported transducer and the readout circuit requires a detailed discussion which is out of the scope of this paper and is planned for the future report. However, in such analysis one must consider the nonlinearity, stray-immunity, offset errors and the noise problem causing an overall error in the measurements. In our design care was taken to minimize the stray capacitances, gap effects, and the environmental effects on the transducer and error sources for the circuit. Although we have tested the readout circuit at the frequency of 10 kHz, the design is capable of operating at frequencies up to 50 kHz. The environmental conditions such as air temperature and humidity effects can influence the capacitance variation, but these minor changes can be compensated for by the zero adjustments at the start of a measurement and are negligible for the short period of the meaurement. Finally, we admit that there are some other methods for the construction of the more accurate micro sensors, but such method of fabrication requires micro machining and micro technology that are not available at the present time.

ACKNOWLEDGMENTS

This work was supported in part by the Sharif University of Technology research program. The authors would like to thank for the grant devoted to this research. The author gratefully acknowledges the technical assistance given by A. Ashrafi.

REFERENCES

1. R. F. Wolffenbutell, K. M. Mahmoud and P. P. L. Regtien, ***IEEE Trans. Instrum. Meas.***, IM-39,(1990) 991-997.
2. S. M. Huang, A. L. Stott, R.G. Green and M. S. Beck, J. ***Phys. E: Sci. Instrum.***, 21, (1988) 242-251.
3. R. F. Wolffenbutell and J. A. Foerster, ***IEEE Trans. Instrum. Meas.***, IM-39,(1990) 1008-1013.
4. S.H. Khan and F. Abdullah IEEE Proceedings-G, 140,(1993) 216-222.
5. J. T. Kung, H. S. Lee, and R. T. Howe, ***IEEE J. Solid State Circuits***, SC-23,(1988) 972-977.
6. J. T. Kung, R. N. Mills and H. S. Lee, ***IEEE Trans. Instrum. Meas.***, IM-42,(1993) 939-943.
7. W. C. Heerens and F. C. Vermeulen, ***J.A Phys.***, 46,(1975) 2486-2490.
8. W. C. Heerens, ***J. Phys. E. : Sci. Instrum.***, 15, (1982), 137-141.
9. A. Ashrafi, MS Thesis, K.N. Toosi University of Technology, Tehran, (1995).
10. R. F. Wolffenbuttell and P. P. L. Regtien, ***IEEE Trans. Instrum. Meas.***, IM-36, (1987) 868-872.
11. H. Golnabi and A. Ashrafi, ***IEEE Trans. Instrum. Meas.***, IM-45, (1996) 312-314.
12. M. H. W. Bonse, F. Zhu and H. F. Van Beek, ***Meas. Sci. Technol.***, 4, (1993), 801-807.
13. S. M. Haung R G. Green A. Plakowski and M. S. Beck, ***IEEE Trans. Instrum. Meas.***, IM-37, (1988), 368-373.
14. J W Schofield, ***J. Phys. E: Sci, Istrum.***, 5, (1972), 822-825.
15. A. Hauneberg, T E Hansen, P A. Ohlckers, E Carlson, B. Dahl and O. Holwech, Sensors and Actuators, 9, (1986), 345.